Pergamon

Int. J. Solids Structures Vol. 32, No. 15, pp. 2245–2256, 1995

0020-7683/95 $9.50 + .00

0020-7683(94)00244-4

AXISYMMETRICAL BUCKLING BEHAVIOR OF TRUNCATED SHALLOW SPHERICAL SHELLS SUBJECTED TO LINE MOMENT LOADS

SHUXIAN GU

Department of Modern Mechanics, University of Science and Technology of China, Hefei 230026, People's Republic of China

(*Received* 14 *September* 1993; *in revised form* 20 *September* 1994)

Abstract—This paper is concerned with the nonlinear stability of simply supported shallow spherical shells with a center hole under the action of a uniformly distributed line moment along a circle concentric with the shell boundary. A set of truncated monomials have been used in representing various discontinuous distributions in order to simplify formulations. We have computed the load–deflection curves, buckling loads, radial membrane forces and the critical geometrical parameter K_c for shells with various center-hole radii. Our numerical results show that (1) both the initial shell stiffness and the buckling load are decreased due to the presence of a center hole with a free boundary. If the hole edge is reinforced with a rigid ring, the truncation not only raises the initial shell stiffness and the buckling load of the shell but also its critical geometrical parameter K_c. The effects of the truncation increase upon increasing the radius of the center hole; (2) for shells with large geometrical parameter K, the radial membrane forces at critical buckling become partly tensional and the buckling load will be almost unaffected by the truncation if the center hole is situated inside the tensile region.

NOMENCLATURE

E	Young's modulus
D	$= Eh^3/12(1-\nu^2)$
K	$= \sqrt{12(1-\nu^2)}(2f/h)$, geometrical parameter
K_c	critical geometrical parameter
M	line moment load per unit length
M_r	radial moment
N_r	radial membrane force
N_θ	circumferential membrane force
$\bar{N}_r$	$= 12(1-\nu^2)a^2 N_r/Eh^3$, dimensionless radial membrane force
a	base radius of shell
b	radius of loaded circle
c	radius of center hole
f	rise height of shell
h	shell thickness
m	$= 12(1-\nu^2)\sqrt{12(1-\nu^2)}\,a^2 M/Eh^4$, dimensionless line moment load
m_c	buckling load
u	horizontal meridional displacement
w	vertical displacement
α	$= b/a$, dimensionless radius of loaded circle
β	$= c/a$, dimensionless radius of center hole
ν	Poisson's ratio

INTRODUCTION

A shallow spherical shell with a center hole is one of the basic structural elements in engineering, and thus it is important to clarify the buckling behavior of the truncated shell under various loading and boundary conditions, in particular the effects of the hole on the buckling behavior. The pioneer works of Budiansky (1959) and Tilman (1970) have given the results of theoretical and experimental investigations of clamped shallow spherical shells

with a center hole under a uniform pressure. The papers of Liu (1965, 1977) and Liu *et al.* (1988) concern the buckling behavior of truncated shallow spherical shells under the action of ring loads or line moments along the hole edge. Recently, we have applied the B-spline approximation to buckling problems of ring-loaded shallow spherical caps (Gu, 1988) and truncated shells (Gu, 1991) and obtained reasonably accurate solutions within a wide range of values of the geometrical parameter K. In this paper we shall discuss the symmetrical large deflections and the buckling behavior of truncated shells that are subjected to a line moment uniformly distributed on a circle concentric with the shell boundary. Apparently, the treatment of such a problem will be more difficult than conventional nonlinear symmetrical buckling problems because we have to find a solution in which the moment distribution is discontinuous, while the shear distribution of the shell remains continuous. Therefore, the purpose of this paper is twofold: (1) to present a method of solving the symmetrical buckling problems of a thin shell in which the moment load is discontinuously distributed; (2) to investigate the buckling behavior of shallow spherical shells with a center hole under the action of a line moment, in particular the effects of the hole on the buckling behavior.

The steps in our analysis are as follows. At first we replace the line moment by a couple of ring loads and let the difference between the radii of the two loaded circles approach zero in subsequent numerical calculations. Then we use a set of truncated monomials $(x-x_i)_+^m$ and $(x-x_i-\Delta x)_+^m$ to separate out the discontinuous components of the irregular distributions so that we only need to manage sufficiently smooth distributions. Finally, we use both successive iterative techniques and the B-spline approximation to solve the nonlinear boundary value problem.

We have computed load–hole edge deflection curves, buckling loads, radial membrane forces and the critical geometrical parameter K_c (geometrical parameter $K=\sqrt{12(1-\nu^2)}(2f/h)$, where f represents the shell rise, h the shell thickness and ν the Poisson's ratio; K_c is the highest value of K below which buckling will never occur). All the calculations were carried out for simply supported truncated spherical shells under the action of line moment loads with various values of load radius α, hole radius β and geometrical parameter K. The results obtained show the following. (1) The initial shell stiffness and the buckling load are decreased due to the presence of the center hole. The effects of truncation on the buckling load and initial shell stiffness increase upon increasing the radius of the center hole. However, when the radius of the center hole is relatively small in comparison with that of the loaded circle, the effect of the center hole on the buckling load decreases rapidly as the geometrical parameter K increases and becomes negligible for sufficiently large K. (2) If the hole edge is reinforced with a rigid ring, not only the initial shell stiffness and the buckling load, but also the critical geometrical parameter K_c, will increase.

In order to understand the foregoing results, we have calculated the radial membrane force N_r and the deflection W as functions of the radial coordinates. From these calculations we note that it is crucial for buckling of a shell that the radial membrane force attains a sufficiently large negative value (negative N_r produces compression in the radial direction) somewhere in the shell. For shells at the critical buckling state, the radial membrane forces are negative everywhere when K is small and become partly positive in the central region of the shell as K increases. Thus, if the center hole is situated inside the central tensile region, the distribution of N_r in the compressive region will be almost unaffected by the truncation. This fact explains why the effect of truncation on the buckling load is negligible for shells with large K and a relatively small center hole.

To test the accuracy of our numerical scheme, we have also investigated the limiting case in which the load radius α approaches 1 and the hole radius approaches zero. For $K<22$, the results obtained coincide with those obtained by other authors for spherical caps subjected to a line moment along the outside edge of the cap (Yeh, 1980). For $K<28$, the results are in good agreement with those obtained by iterative techniques in sixth-order approximation. For $32<K<400$, we still obtain fairly good convergent results, while the results obtained by iterative techniques fail to converge in numerical calculations.

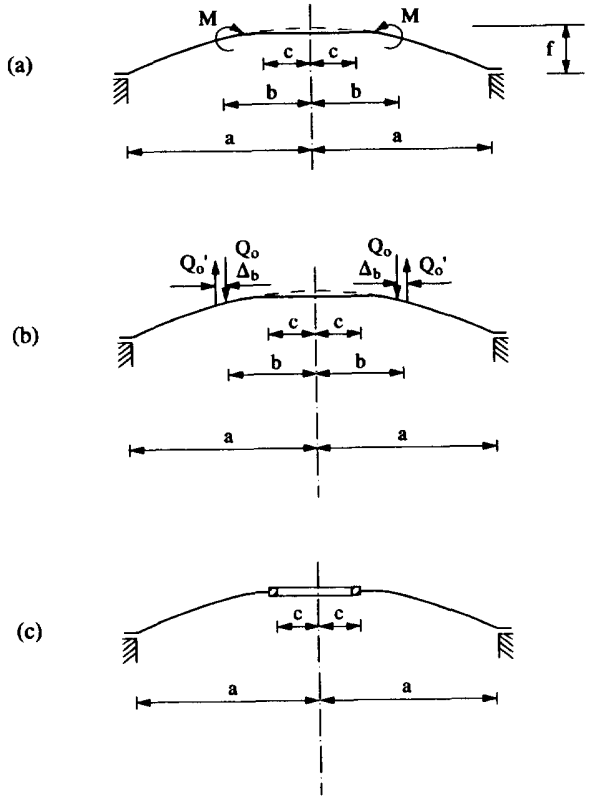

Fig. 1. A truncated spherical shell segment: (a) and (b) center hole with free boundary; (c) center hole reinforced with a rigid ring.

FUNDAMENTAL EQUATIONS AND BOUNDARY CONDITIONS

The stability problem for a shallow spherical shell subjected to a line moment load is harder to cope with than conventional nonlinear stability problems because of the discontinuity of distribution of moment and the continuity of distribution of shear. Here we replace the line moment by a pair of ring loads (Q_0 and Q_0') which are equivalent to the line moment (see Fig. 1). According to the equivalence principle of force, we have $Q_0 = M/\Delta b$ and $Q_0' = bQ_0/(b+\Delta b)$, where M represents the intensity of the line moment and Q_0 and Q_0' the intensities of the inner and outer ring loads, respectively.

The equations of the finite symmetrical deflections of a shallow spherical shell with a center hole subjected to a set of ring loads shown in Fig. 1(b) can be expressed in the form [see e.g. Feodosiev (1949) or Hu (1954)]

$$Dr\frac{\mathrm{d}}{\mathrm{d}r}\left(\frac{1}{r}\frac{\mathrm{d}}{\mathrm{d}r}\left(r\frac{\mathrm{d}w}{\mathrm{d}r}\right)\right) = rN_r\left(\frac{2f}{a^2}r+\frac{\mathrm{d}w}{\mathrm{d}r}\right)+(r-b)_+^0\,Q_0b-(r-b-\Delta b)_+^0\,Q_0b \tag{1}$$

$$\frac{r}{Eh}\frac{\mathrm{d}}{\mathrm{d}r}\left(\frac{1}{r}\frac{\mathrm{d}}{\mathrm{d}r}(r^2N_r)\right) = -\frac{\mathrm{d}w}{\mathrm{d}r}\left(\frac{2f}{a^2}r+\frac{1}{2}\frac{\mathrm{d}w}{\mathrm{d}r}\right), \tag{2}$$

where r represents the distance from the axis of symmetry, w the vertical displacement, N_r the radial membrane force, $D = Eh^3/12(1-\nu^2)$ and $(r-b)_+^0$, $(r-b-\Delta b)_+^0$ are truncated monomials defined by

$$X_+^m = \begin{cases} X^m & \text{for } X \geqslant 0 \\ 0 & \text{for } X < 0 \end{cases}, \quad m = 1, 2, \ldots, \tag{3a}$$

$$X_+^0 = \begin{cases} 1 & \text{for } X > 0 \\ 0 & \text{for } X < 0. \end{cases} \tag{3b}$$

We see that X_+^m is a function with continuous derivatives up to the $(m-1)$th order but its mth-order derivative has a jump at $X = 0$.

Now noting that, for shallow thin spherical shells, the radial moment M_r, circumferential membrane force N_θ and the horizontal meridional displacement u can be written as (Hu, 1954)

$$M_r = -D\left(\frac{d^2w}{dr^2} + \frac{v}{r}\frac{dw}{dr}\right),$$

$$N_\theta = N_r + r\frac{dN_r}{dr},$$

$$u = \frac{r}{Eh}\left[(1-v)N_r + r\frac{dN_r}{dr}\right],$$

the boundary conditions for a truncated shell with a simply supported outside edge and free hole edge are

$$w = 0, \quad N_r = 0, \quad -D\left(\frac{d^2w}{dr^2} + \frac{v}{r}\frac{dw}{dr}\right) = 0 \quad \text{at} \quad r = a, \tag{4a}$$

$$w, \quad \frac{dw}{dr}, \quad N_r, \quad M_r \quad \text{and} \quad \frac{dN_r}{dr} \quad \text{are continuous} \quad \text{at} \quad r = b, \tag{4b}$$

$$w, \quad \frac{dw}{dr}, \quad N_r, \quad M_r \quad \text{and} \quad \frac{dN_r}{dr} \quad \text{are continuous,} \quad \text{at} \quad r = b + \Delta b \tag{4c}$$

$$N_r = 0, \quad -D\left(\frac{d^2w}{dr^2} + \frac{v}{r}\frac{dw}{dr}\right) = 0 \quad \text{at} \quad r = c. \tag{4d}$$

After introducing dimensionless quantities defined by

$$\rho = \frac{r}{a}, \quad W = \sqrt{12(1-v^2)}\frac{w}{h}, \quad \varphi = -\frac{dW}{d\rho} - K\rho, \quad K = \sqrt{12(1-v^2)}\frac{2f}{h},$$

$$P = \frac{12(1-v^2)\sqrt{12(1-v^2)}}{Eh^4}a^2bQ_0, \quad S = \frac{12(1-v^2)a^2}{Eh^3}\rho N_r,$$

$$m = \frac{12(1-v^2)\sqrt{12(1-v^2)}}{Eh^4}a^2M, \quad \alpha = \frac{b}{a}, \quad \beta = \frac{c}{a}, \quad \Delta\alpha = \frac{\Delta b}{a}$$

and noting that $m = P(\Delta\alpha/\alpha)$, we can rewrite eqns (1) and (2) as

$$\rho\frac{d}{d\rho}\frac{1}{\rho}\frac{d}{d\rho}\rho\varphi = S\varphi - (\rho-\alpha)_+^0 P + (\rho-\alpha-\Delta\alpha)_+^0 P, \tag{5}$$

$$\rho\frac{d}{d\rho}\frac{1}{\rho}\frac{d}{d\rho}\rho S = \tfrac{1}{2}(K^2\rho^2 - \varphi^2), \tag{6}$$

and the boundary conditions (4a), (4b), (4c) and (4d) as

$$W = 0, \quad S = 0, \quad \frac{d\varphi}{d\rho} + \frac{v}{\rho}\varphi = -K - Kv, \quad \text{at} \quad \rho = 1, \tag{7a}$$

$$W, \quad \varphi \quad \text{and} \quad \frac{d\varphi}{d\rho} \quad \text{are continuous,} \quad \text{at} \quad \rho = \alpha, \tag{7b}$$

$$W, \quad \varphi \quad \text{and} \quad \frac{d\varphi}{d\rho} \quad \text{are continuous,} \quad \text{at} \quad \rho = \alpha + \Delta\alpha, \tag{7c}$$

$$S = 0, \quad \frac{d\varphi}{d\rho} + \frac{v}{\rho}\varphi = -K - Kv, \quad \text{at} \quad \rho = \beta. \tag{7d}$$

If the hole edge is reinforced with a rigid ring, condition (7d) must be replaced by

$$\varphi = -K\beta, \quad \rho\frac{dS}{d\rho} - vS = 0, \quad \text{at} \quad \rho = \beta. \tag{7d'}$$

To circumvent the convergence difficulties encountered in solving the boundary value problem (5)–(7) when the nonlinear terms in eqns (5) and (6) become dominant, we carried out the incremental iterative techniques as follows.

Assuming that the solution of eqns (5)–(7) at a given load $P = P_n$ is known and can be written as $\varphi = \varphi_n$, $S = S_n$ and $W = W_n$, let the solution at $P = P_n + \Delta P_n$ be expressed by $\varphi = \varphi_n + \Delta\varphi_n$, $S = S_n + \Delta S_n$, $W = W_n + \Delta W_n$. Then, from eqns (5)–(7) we obtain

$$\rho\frac{d}{d\rho}\frac{1}{\rho}\frac{d}{d\rho}\rho\Delta\varphi_n = S_n \cdot \Delta\varphi_n + \Delta\varphi_n \cdot \Delta S_n + \Delta S_n \cdot \varphi_n - (\rho - \alpha)_+^0 \cdot \Delta P_n + (\rho - \alpha - \Delta\alpha)_+^0 \cdot \Delta P_n, \tag{8}$$

$$\rho\frac{d}{d\rho}\frac{1}{\rho}\frac{d}{d\rho}\rho\Delta S_n = \tfrac{1}{2}(-2\varphi_n \cdot \Delta\varphi_n - (\Delta\varphi_n)^2), \tag{9}$$

$$\Delta W_n = 0, \quad \Delta S_n = 0, \quad \frac{d\Delta\varphi_n}{d\rho} + \frac{v}{\rho}\Delta\varphi_n = 0 \quad \text{at} \quad \rho = 1, \tag{10a}$$

$$\Delta W_n, \quad \Delta\varphi_n, \quad \frac{d}{d\rho}\Delta\varphi_n \quad \text{are continuous} \quad \text{at} \quad \rho = \alpha, \tag{10b}$$

$$\Delta W_n, \quad \Delta\varphi_n, \quad \frac{d}{d\rho}\Delta\varphi_n \quad \text{are continuous} \quad \text{at} \quad \rho = \alpha + \Delta\alpha, \tag{10c}$$

$$\Delta S_n = 0, \quad \frac{d}{d\rho}\Delta\varphi_n + \frac{v}{\rho}\Delta\varphi_n = 0 \quad \text{at} \quad \rho = \beta. \tag{10d}$$

Thus, the solution at an arbitrary load P can be obtained by starting from the known solution at $P = 0$ (i.e. $\varphi = \varphi_0 = -k\rho$, $S = S_0 = 0$, $W = W_0 = 0$) and solving the boundary value problem (8)–(10) successively: $\varphi = -K\rho + \Sigma_n \Delta\varphi_n$, $S = \Sigma_n \Delta S_n$, $W = \Sigma_n \Delta W_n$.

It is evident from eqn (8) and boundary conditions (10b) and (10c) that although $\Delta\varphi_n$ and its derivative $(d/d\rho)\Delta\varphi_n$ are continuous functions of ρ, the second-order derivative $(d^2/d\rho^2)(\rho\Delta\varphi_n)$ will have a jump at $\rho = \alpha$ and $\rho = \alpha + \Delta\alpha$. Therefore it is convenient to introduce a new function $\Delta\varphi_n^*$ defined by

$$\Delta\varphi_n = \Delta\varphi_n^* - \frac{(\rho-\alpha)_+^2}{2!\rho}\Delta P_n + \frac{(\rho-\alpha-\Delta\alpha)_+^2}{2!\rho}\Delta P_n, \tag{11}$$

where $(\rho-\alpha)_+^2$, $(\rho-\alpha-\Delta\alpha)_+^2$ are truncated monomials defined in eqns (3a). Substituting eqn (11) into eqns (8)–(10), we obtain

$$\rho\frac{\mathrm{d}}{\mathrm{d}\rho}\frac{1}{\rho}\frac{\mathrm{d}}{\mathrm{d}\rho}\rho\Delta\varphi_n^* = -\frac{1}{\rho}(\rho-\alpha)_+^1\Delta P_n + \frac{1}{\rho}(\rho-\alpha-\Delta\alpha)_+^1\Delta P_n + S_n\Delta\varphi_n^* - \frac{(\rho-\alpha)_+^2}{2!\rho}\Delta P_n\cdot S_n + \frac{(\rho-\alpha-\Delta\alpha)_+^2}{2!\rho}\Delta P_n\cdot S_n + \Delta S_n \times\left[\Delta\varphi_n^* - \frac{(\rho-\alpha)_+^2}{2!\rho}\Delta P_n + \frac{(\rho-\alpha-\Delta\alpha)_+^2}{2!\rho}\Delta P_n + \varphi_n\right], \tag{12}$$

$$\rho\frac{\mathrm{d}}{\mathrm{d}\rho}\frac{1}{\rho}\frac{\mathrm{d}}{\mathrm{d}\rho}\rho\Delta S_n = -\varphi_n\left[\Delta\varphi_n^* - \frac{(\rho-\alpha)_+^2}{2!\rho}\Delta P_n + \frac{(\rho-\alpha-\Delta\alpha)_+^2}{2!\rho}\Delta P_n\right] - \frac{1}{2}\left[\Delta\varphi_n^* - \frac{(\rho-\alpha)_+^2}{2!\rho}\Delta P_n + \frac{(\rho-\alpha-\Delta\alpha)_+^2}{2!\rho}\Delta P_n\right]^2, \tag{13}$$

$$\frac{\mathrm{d}}{\mathrm{d}\rho}(\Delta\varphi_n^*) + \frac{v}{\rho}\Delta\varphi_n^* = (1-\alpha)\cdot\Delta P_n - (1-\alpha-\Delta\alpha)\cdot\Delta P_n - (1-v)\frac{(1-\alpha)^2}{2}\Delta P_n + (1-v)\frac{(1-\alpha-\Delta\alpha)^2}{2}\Delta P_n, \quad \Delta W_n = 0, \quad \Delta S_n = 0 \quad \text{at} \quad \rho = 1, \tag{14a}$$

$$\frac{\mathrm{d}}{\mathrm{d}\rho}\Delta\varphi_n^* + \frac{v}{\rho}\Delta\varphi_n^* = 0, \quad \Delta S_n = 0 \quad \text{at} \quad \rho = \beta. \tag{14b}$$

Since the discontinuous terms $(\rho-\alpha)_+^0\Delta P_n$, $(\rho-\alpha-\Delta\alpha)_+^0\Delta P_n$ which appeared in the right-hand side of eqn (8) have been eliminated in eqn (12), the solutions $\Delta\varphi_n^*$ and ΔS_n of the boundary value problem (12)–(14) will have continuous derivatives up to the second order.

SOLUTION FOR THE BOUNDARY VALUE PROBLEM

Equations (12) and (13) represent a set of nonlinear differential equations with variable coefficients, which can be solved only by numerical methods. In contrast to the conventional incremental method, which uses linear approximations of eqns (12) and (13), we solve the nonlinear equations (12)–(13) directly by an iterative method. Moreover, we shall use cubic B-spline functions as test functions and try to fit the solution by dividing the whole interval $[\beta, 1]$ of ρ into N equal parts. Denoting the end points and points of division with numbers $0, 1, 2, \ldots, N$ and letting $t = (1-\beta)/N$, the radial coordinate for the ith point is $\rho_i = \beta + it$. Adding two extra points on both sides of the interval at equal distance t, we assume that the increments $\Delta\varphi_n^*$ and ΔS_n satisfy

$$\Delta\varphi_n^* = \sum_{j=-1}^{N+1} B_j\Omega_3\left(\frac{\rho-\rho_j}{t}\right), \tag{15}$$

$$\Delta S_n = \sum_{j=-1}^{N+1} C_j\Omega_3\left(\frac{\rho-\rho_j}{t}\right), \tag{16}$$

where $\{B_j\}$, $\{C_j\}$ $(j=-1,0,1,\ldots,N+1)$ are undetermined coefficients and $\Omega_3(\rho-\rho_j)/t$ represents the cubic B-spline (Ahlberg *et al.*, 1967). After substituting eqns (15) and (16) into eqns (12)–(14), we obtain $2(N+3)$ independent nonlinear algebraic equations. Solving these algebraic equations by iterative techniques we obtain $\{B_j\}$ and $\{C_j\}$. The increments $\Delta\varphi_n^*$, ΔS_n and $\Delta\varphi_n$ can be readily obtained from eqns (11), (15) and (16), respectively.

NUMERICAL RESULTS AND DISCUSSIONS

We have computed the load–deflection curves, buckling loads, radial membrane forces and the critical geometrical parameter K_c for simply supported shallow spherical shells with various values of load radius α and hole radius β. The accuracy of our numerical calculation is guaranteed by controlling the increments of hole edge deflection ΔW_m (or the increments of load ΔP_n) such that after five iterations the relative error of corresponding load increments (or corresponding hole edge deflection increments) $\eta = |((\Delta P_n)_5 - (\Delta P_n)_4)/(\Delta P_n)_5|$ is kept within a fixed small interval. Moreover, to avoid the divergence which occurs as soon as dW_m/dP or dP/dW_m approaches infinity, the deflection increments and the load increments have been used alternatively as iterative parameters. Besides, we have chosen a set of values of allowed interval of η, the number of dividing points N and the distance $\Delta\alpha(\Delta\alpha = \Delta b/a)$ to test the reliability of our numerical calculations. The results indicate that when $\eta < 10^{-5}$, $N > 100$ and $\Delta\alpha < 0.006$, the solutions are virtually independent of these parameters.

Our results can be summarized as follows.

1. Figure 2(a) and (b) shows calculated buckling loads m_c versus the geometrical parameter K for simply supported truncated shells with fixed load radius $\alpha = 0.5$ and 0.7 and with various hole radii β. These results show that, in general, the buckling load m_c decreases due to the presence of the center hole and the effect of the center hole increases when the hole radius increases. For relatively small center hole radii (in comparison with the radius of the loaded circle) the effects of the center hole on m_c decrease rapidly as the geometrical parameter K increases and become negligible for sufficiently large K. For example, for $\alpha = 0.7$ and $\beta \leqslant 0.4$, the effect of the center hole becomes negligible when

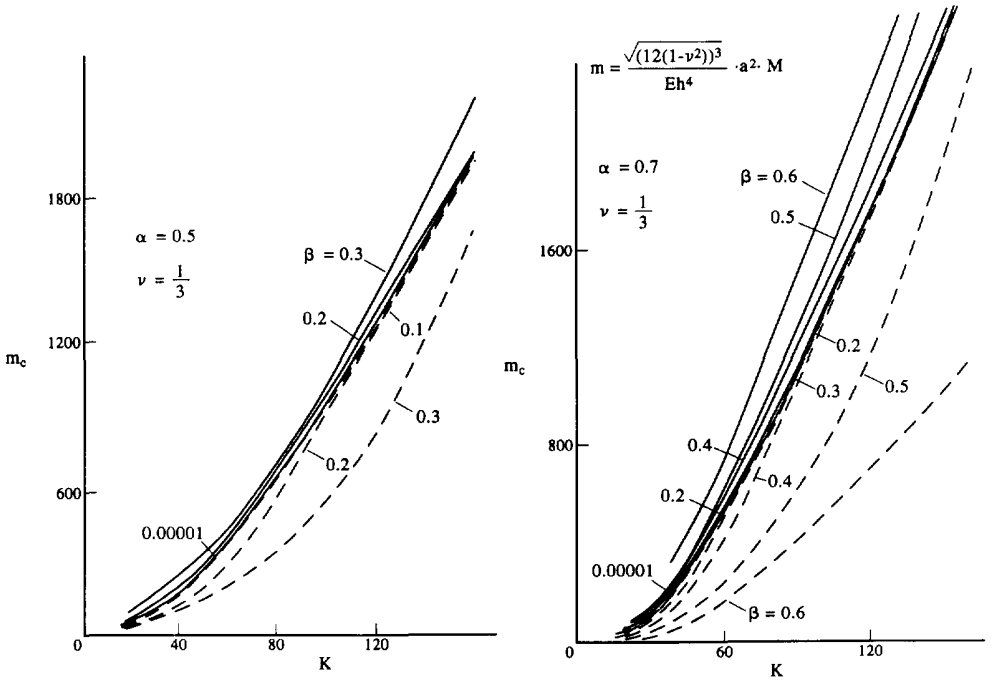

Fig. 2. Buckling load m_c versus geometrical parameter K for simply supported spherical shells with center hole of various radii β and fixed load radii α: (a) $\alpha = 0.5$; (b) $\alpha = 0.7$. Solid curves are for a hole reinforced with a rigid ring and dashed curves for a hole with a free edge.

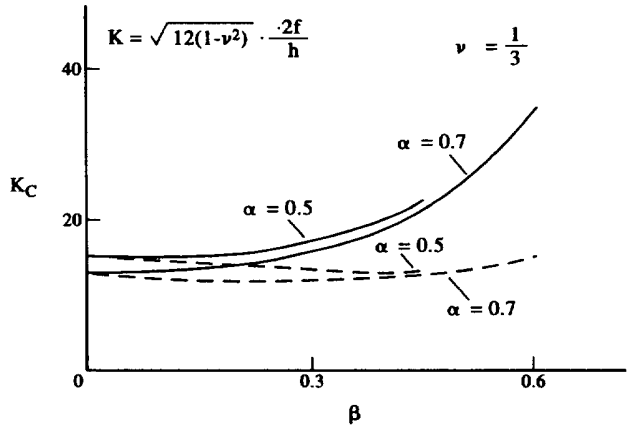

Fig. 3. Critical geometrical parameter K_c versus center hole radius β with fixed load radius α (solid curves for rigid hole edge, dashed curves for free hole edge).

$K > 96$, while for $\alpha = 0.5$ and $\beta \leqslant 0.2$ the effect becomes negligible when $K > 100$. However, if the hole edge is reinforced with a rigid ring (note that there are two types of curve in Figs 2–6: solid curves for holes with a rigid ring and dashed curves for holes with a free edge), not only can the buckling load be raised but so can the critical geometrical parameter K_c.

2. In Fig. 3 we have plotted the critical geometrical parameter K_c versus the radius of the center hole β for simply supported shells with a fixed load radius ($\alpha = 0.5$ and 0.7). This figure shows that K_c depends only slightly upon β when the hole edge is free. If the hole edge is reinforced with a rigid ring, K_c will be remarkably increased for shells with large hole radii.

3. Figure 4 shows the load–hole edge deflection curves for shells with various hole radii ($\alpha = 0.7$, $K = 24$). From this figure we see that when the hole edge is free, the initial

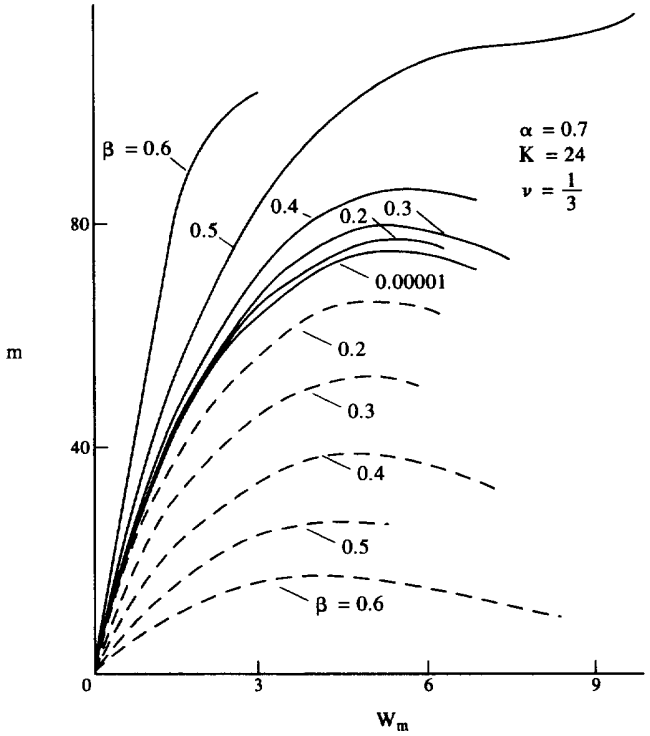

Fig. 4. Load-hole edge deflection curves of simply supported spherical shells with various center hole radii β and fixed load radius α (solid curves for rigid hole edge, dashed curves for free hole edge).

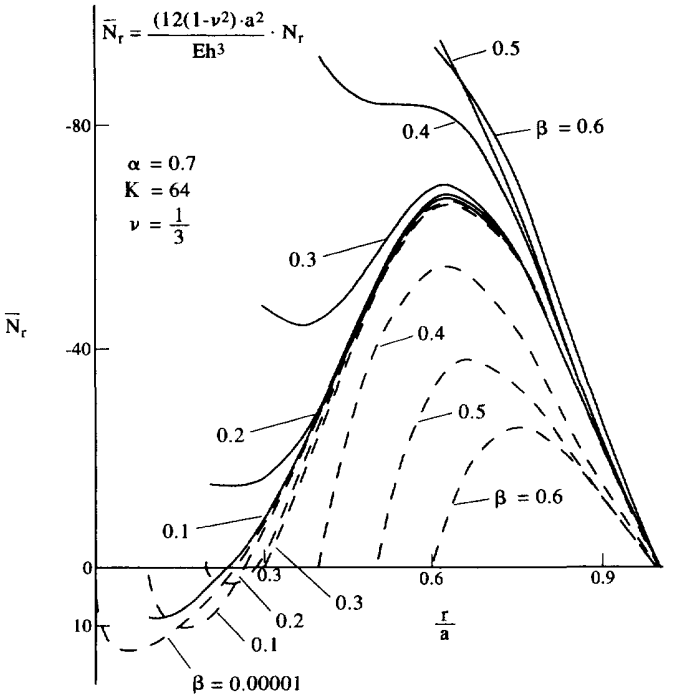

Fig. 5. Radial membrane force $\bar{N}_r$ ($\bar{N}_r = 12(1-\nu^2)a^2N_r/Eh^2$) of a simply supported spherical shell with various center hole radii β under the action of buckling load for $\alpha = 0.7$, $K = 64$ (solid curves for rigid hole edge, dashed curves for free hole edge).

shell stiffness decreases upon increasing the hole radius, whereas when the hole edge is reinforced with a rigid ring, the initial shell stiffness increases upon increasing the hole radius. The same conclusion has been obtained for shells with $\alpha = 0.7$ and $K = 64$.

4. In order to see more clearly the effect of a center hole on the buckling behavior of a simply supported shell, we computed the dimensionless radial membrane forces and the dimensionless deflection surfaces as functions of radial coordinates under the action of a buckling load. The results are shown in Fig. 5 (radial membrane force) and Fig. 6 (deflection surface) for $\alpha = 0.7$, $K = 64$. We also computed the case for $\alpha = 0.7$, $K = 24$, and it is interesting to note that the radial membrane forces are negative everywhere (i.e. compressive) when $K = 24$ and become partly positive (i.e. tensional) when $K = 64$ (Fig. 5). Furthermore, we found that, in the latter case, the distribution of the radial membrane forces in the compressive region is almost unaffected by the truncation if the radius of the center hole does not exceed the radius of the tensile region.

5. Figure 7 shows the radial membrane forces for a simply supported shell with a center hole reinforced by a rigid ring when $\alpha = 0.7$, $\beta = 0.5$ and $K = 24$. Since in this case we have $K < K_c$ (cf. Fig. 3), the shell will never buckle. Thus we plotted in Fig. 7 several curves for different loading conditions to show the changes of radial membrane forces when the load increases. We see that when the load is small the radial membrane forces are compressive everywhere and their absolute value increases upon increasing the load. As the load increases further, the absolute values of the radial membrane forces begin to decrease until the radial membrane forces become tensional everywhere. From this we may conclude that it is necessary for the buckling of a shell that the radial membrane force is compressive and attains a sufficiently large value somewhere in the shell.

6. Table 1 shows the calculated buckling loads when β approaches zero and α approaches unity. For the simply supported shells with two different boundary conditions at the hole edge (free or reinforced with a rigid ring) the limiting results obtained are just the same and coincide well with those obtained by other authors for spherical caps with $K < 22$ (Yeh *et al.*, 1980).

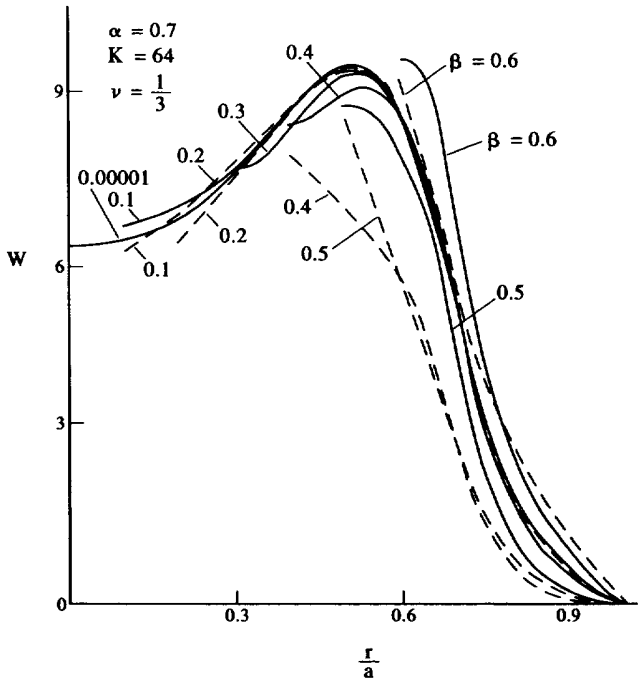

Fig. 6. Deflection curves of a simply supported spherical shell under buckling load with various center hole radii β for fixed $\alpha = 0.7$, $K = 64$ (solid curves for rigid hole edge, dashed curves for free hole edge).

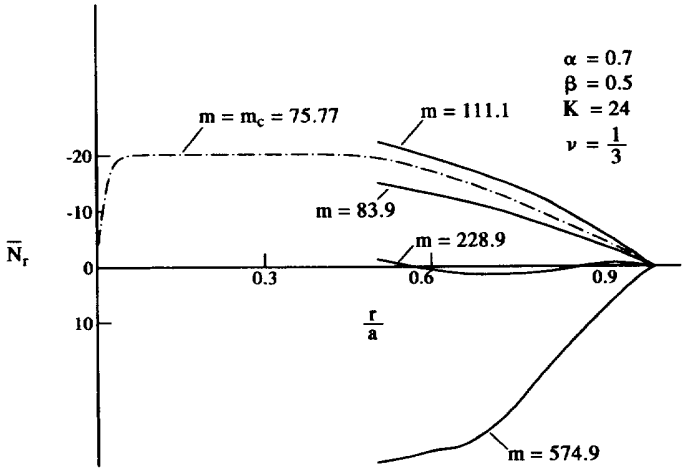

Fig. 7. Radial membrane force $\bar{N}_r$ of a simply supported spherical shell with a center hole reinforced with a rigid ring under various moment loads m. Dashed curve represents the $\bar{N}_r$ under buckling load m_c when the radius of center hole approaches zero.

7. Figure 8 shows the critical geometrical parameter K_c versus the radius of loaded circle α for spherical caps. From this figure we observe that K_c increases monotonously with the decrement of α. For $\alpha > 0.7$ the changes in K_c are unremarkable, whereas for $\alpha < 0.45$, K_c increases rapidly as α decreases (e.g. when $\alpha = 0.15$, K_c can be as high as 306.9).

CONCLUSIONS

From the present study the following conclusions have been drawn.

(1) The initial stiffness and the buckling load are decreased due to the presence of a center hole with a free edge, but they can be increased by reinforcing the hole edge with a rigid ring.

Table 1. Buckling loads m_c for simply supported shallow thin spherical shell subjected to line moment along the outside edge

$$m_c\left(m=\frac{12(1-\nu^2)\sqrt{12(1-\nu^2)}\cdot a^2}{Eh^4}M,\quad M=Q_0\Delta b,\quad \nu=\frac{1}{3}\right)$$

		Iterative techniques		Present results	
K	(Yeh, 1980) Third approximation	Fifth approximation	Sixth approximation	$\alpha = 0.9999$ $\Delta\alpha = 0.00001$	$\alpha = 0.998$ $\Delta\alpha = 0.001$
14	19.377	19.3456	19.3442	19.3129	19.368
16	24.346	24.2336	24.2268	24.1911	24.268
18	30.593	30.2694	30.2560	30.1820	30.278
20	38.049	37.2000	37.1730	37.1082	37.214
22	46.608	44.7681	44.7580	44.6976	44.815
24	56.089	52.9066	52.8331	52.7401	52.890
26	66.249	61.5725	61.0213	61.1025	61.276
28	76.831	70.9605	69.7222	69.7357	69.943
300				3152.72	3161.63
400				4924.09	4938.09

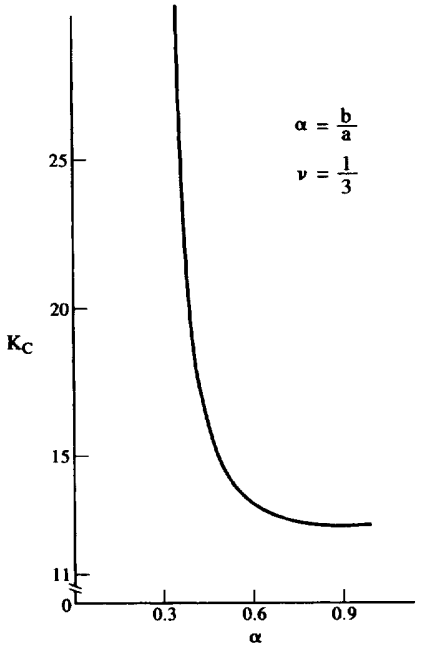

Fig. 8. Critical geometrical parameter K_c versus line moment load radius α for a truncated shell when the radius of the center hole approaches zero.

(2) It is necessary for the buckling of a shell that the radial membrane force is compressive and attains a sufficiently large value somewhere in the shell. For caps with large geometrical parameter K, the radial membrane forces at critical buckling state become tensional in a central region of the cap. The buckling load will be almost unaffected by the truncation if the radius of the center hole is less than the radius of the tensile region.

(3) When the load radius α decreases, the critical geometrical parameter K_c of a spherical cap increases rapidly as soon as $\alpha < 0.45$ and the instability caused by the line moment load is no longer of practical interest when the dimensionless load radius α is less than 0.3 (cf. Fig. 8).

REFERENCES

Ahlberg, J. H., Nilson, E. N. and Walsh, J. L. (1967). *The Theory of Spline and their Applications.* Academic Press, New York.

Budiansky, B. (1959). Buckling of clamped shallow spherical shells. *Proc. IUTAM Symp. on the Theory of Thin Elastic Shells*, pp. 64–94. North Holland, Amsterdam.

Feodosiev, V. I. (1949). *Elastic Elements in Precision Instrument Engineering* (in Russian). Oborongiz, Moscow.

Gu, Shu-xian (1988). Nonlinear stability of large K-value shallow spherical shells with a symmetrically distributed line load. *Acta Mechanica Solida Sinica* **1,** 369–381.

Gu, Shu-xian (1991). Buckling behavior of ring-loaded shallow spherical shells with a center hole. *Int. J. Non-Linear Mech.* **26,** 263–274.

Hu, Hai-chang (1954). On the snapping of a thin spherical cap. *Wuli Xuebao* (in Chinese) **10,** 105–136.

Liu, Ren-huai (1965). Nonlinear stability of truncated shallow spherical shells with uniform moment load at hole edge. *Kexue Tongbao* (in Chinese) **3,** 253–255.

Liu, Ren-huai (1977). Axisymmetrical stability of truncated shallow spherical shells with line load at hole edge. *Mechanics* (in Chinese) **3,** 206–212.

Liu, Ren-huai (1988). On the nonlinear stability of a truncated shallow spherical shell under a concentrated load. *Appl. Math. and Mech.* (in Chinese) **9,** 95–105.

Tilman, S. C. (1970). On the buckling behavior of shallow spherical caps under a uniform pressure load. *Int. J. Solids Struct.* **6,** 37–52.

Yeh, Kai-yuan *et al.* (1980). Nonlinear stability of a shallow spherical cap under the action of uniform edge moment. *Appl. Math. and Mech.* (in Chinese) **1,** 71–87.